

# Processing-morphology relationships of compatibilized polyolefin/polyamide blends

## Part II *The emulsifying effect of an ionomer compatibilizer as a function of blend composition and viscosity ratio*

J. M. WILLIS, V. CALDAS, B. D. FAVIS\*

*Industrial Materials Institute, National Research Council of Canada, Boucherville, Quebec, Canada J4B 6Y4*

The emulsifying effect of a polyethylene-based ionomer on the phase size/composition relationship was studied for polypropylene/polyamide and polyethylene/polyamide blends. The particle size measured for the uncompatibilized blends increased with minor phase concentration, particularly as the region of dual phase continuity was approached. This relationship was less pronounced when ionomer was added, and the dimensions of the dispersed phase were significantly reduced. A narrowing of the region of dual phase continuity was observed due to the addition of ionomer. An increase in the torque measured during melt blending in a Brabender mixing chamber resulted when ionomer was added, due to the increase in the interactions at the interface. The particle size determined for the uncompatibilized blends increased with viscosity ratio. The effect was also less pronounced for the compatibilized blends. From these observations, it was possible to conclude that the effect of interfacial modification on morphology predominates over that of composition and viscosity ratio. The effects were interpreted in terms of the reduction of interfacial mobility due to the compatibilization.

### 1. Introduction

The control of the size and shape of the dispersed phase in a polymer blend has been gaining considerable attention of late. It is an important area of blending technology since it is the morphology of the blend which relates its properties to the manner in which the blend was processed.

Several examples of the practical application of morphological control can be found in the literature. It is possible to improve the impact strength of a blend by adequately controlling the size [1-7] and size distribution [8-10] of the dispersed phase. This effect has resulted in the commercial success of such blends as high-impact polystyrene (HIPS) and acrylonitrile/butadiene/styrene (ABS), manufactured by emulsion polymerization [11-14]. Impact modification can also be achieved through the melt blending of thermoplastics with elastomeric materials [1-3, 15-18]. The shape of the minor phase is also highly dependent on the processing conditions. Plate-like or laminar morphologies have been found during blow moulding [19] and sheet extrusion [20] processes. Subramanian

*et al.* [21-23] and Kamal *et al.* [24] have shown that blends which are characterized by such laminar morphologies may exhibit good barrier properties.

The principal parameters which govern the dispersed phase size and shape include: (i) the shear rate (shear stress) applied to the blend during mixing, (ii) the composition of the blend, (iii) the interfacial tension, (iv) the viscosity ratio or torque ratio (ratio of the torque of the dispersed phase to that of the matrix), (v) the elasticity of the components, and (vi) processing parameters such as time of mixing, mode of addition of the compatibilizer, etc. In our laboratory, the influence of several of these parameters has been studied quantitatively using an immiscible blend, polypropylene/polycarbonate [25-27]. The aspect of interfacial modification has also been addressed using polyolefin/polyamide blends [28, 29]. Uncompatibilized polyethylene/polyamide blends are immiscible, and as such are characterized by two distinct phases [30, 31]. Polyolefin/polyamide blends can be rendered compatible by the addition of a polyethylene-based ionomer during melt blending [28, 29]. This ternary poly-

© Government of Canada, National Research Council Canada. Reproduced with permission of the Minister of Supply and Services, Canada, 1991.

\*Address to whom correspondence should be sent,

Present address: Ecole Polytechnique de Montreal, Department of Chemical Engineering, Montreal, Quebec, Canada, P.O. Box 6079, Stn. A, H3C 3A7.

olefin/ionomer/polyamide blend system is of interest because of its potential applicability in industry [32, 33].

The overall objective of this work is the quantitative analysis of the influence of composition and viscosity (torque) ratio on the morphology of compatibilized polypropylene/polyamide and polyethylene/polyamide blends. The effects are interpreted in terms of the reduction of interfacial mobility due to the compatibilization.

## 2. Experimental procedure

### 2.1. Resin characterization

The polypropylene resins used in this study were Pro-fax 6301 (PP-1), 6501 (PP-2) and 6701 (PP-3), received from Himont in powdered form. These resins were compounded with an antioxidant, Irganox 1076 (Ciba-Geigy), on a twin screw extruder and transformed into pellets. The high-density polyethylene resins, 07055C (PE-1), 36056 (PE-2) and 05054C (PE-3) were obtained from Dow as pellets. The polyamide-6 resins, Zytel 211 (PA-1) from Dupont, and Capron 8200 (PA-2) and Capron 8202 (PA-3) from Allied, were also obtained in the form of pellets. The ionomer used in this study, Surlyn 9020 obtained from Dupont, is a random terpolymer consisting of roughly 80% polyethylene and 20% of a mixture of methacrylic acid and isobutyl acrylate. The exact proportion of this mixture is unknown. The methacrylic acid is partially neutralized with zinc to approximately 70%.

Some properties obtained for these resins are given in Table I. It was possible to determine the torque of each resin by mixing 60 ml of the resin in the Brabender mixing chamber at 250 °C for 5 min with the rotors turning at 50 revolutions per minute (r.p.m.). The torque (Nm) represents a measure of the work required to turn the rotors in the mixing chamber.

### 2.2. Compounding

The resins were dry blended and dried under vacuum at 95 °C overnight. Blend compositions are given in the text in terms of weight fraction.

The mixed pellets were melt blended in the Brabender mixing chamber using the roller blades recommended for high shear applications. A typical

blending experiment consisted of the following steps. The resin mixture was fed into the mixing chamber initially set at 250 °C, while the blades were turning at 50 r.p.m. Once all of the resin was added, the blend was allowed to mix for 5 min under a constant flow of dry nitrogen. At the end of 5 min, the melt was rapidly transferred to a mould which was then held in a hydraulic press under 2.5 MPa of pressure until the sample had cooled down to room temperature (approximately 3 min). The morphology of a blend prepared in this manner was found to be identical to that observed for a blend which was simply removed from the mixing chamber and rapidly quenched in ice water.

### 2.3. Scanning electron microscopy

The freeze-fractured surfaces were prepared by first immersing a small rectangular strip of each sample in liquid nitrogen for 10–15 min prior to fracturing. For the microtomed samples, rectangular specimens were cut from the moulded blend samples to have dimensions of roughly 1 × 1.5 × 0.5 cm. A Reichert Jung Supercut 2050 microtome equipped with a diamond knife was used to prepare plane surfaces for each specimen. Prior to microtoming, each sample was frozen in liquid nitrogen. While cutting, the surface of the sample was held at approximately –100 °C to reduce the degree of surface deformation.

The microtomed samples were then treated with a suitable solvent to dissolve the minor phase present at the surface of the specimen. For the polyamide minor phase, this procedure consisted of soaking the specimen in *m*-cresol at room temperature for four days. To dissolve the polyolefin minor phase, the specimens were heated in decalin at 120 °C for 1 h.

The fractured and microtomed/etched surfaces of each blend were then examined under a Jeol model 35-CF scanning electron microscope (SEM) operating at 10–15 kV.

### 2.4. Image analysis

The semi-automatic image analyser used to measure the diameters of the dispersed phase was developed in-house. The operation of this instrument has been described elsewhere [25]. For each sample, approximately 200 to 500 diameter measurements were

TABLE I Properties of the polypropylene, high-density polyethylene, polyamide-6 and Surlyn ionomer resins

Resin	Melt index (g/10 min)	Density @ 250 °C (g/ml)	Torque @ 250 °C <sup>a</sup> (Nm)
PP-1	11.0	0.75	5.2
PP-2	4.0	0.75	8.6
PP-3	1.0	0.75	12.6
PE-1	7.0	0.74	5.9
PE-2	0.4	0.74	18.0
PE-3	5.3	0.74	6.9
PA-1	—	0.96	8.6
PA-2	—	0.96	9.8
PA-3	—	0.96	5.7
IONOMER	1.0	0.74	14.3

<sup>a</sup> For 5 minutes of mixing in Brabender mixing chamber.

obtained from the SEM photomicrographs of the microtomed surfaces. Number average diameters,  $d_n$ , volume average diameters,  $d_v$ , and the polydispersity,  $P_d (= d_v/d_n)$ , were then calculated. A correction factor was applied to the diameters determined from the microtomed surfaces [5].

### 3. Results and discussion

#### 3.1. Effect of blend composition on morphology

The size of the dispersed phase in the uncompatibilized PP-2/PA-1 blends was determined from the SEM photomicrographs of the microtomed surfaces shown in Fig. 1, and the results presented in Fig. 2a. As the concentration of the minor phase increases, larger particle sizes are observed. These trends have previously been observed by other authors [25, 34–38] for a variety of immiscible blends. Moreover, the data for the PP-2/PA-1 blend given in Table II indicate that the dispersity ( $d_v/d_n$ ) of the particle size increases with composition. This effect is due to the greater probability of phase contacts or particle–particle interactions during the mixing process.

The dimensions of the dispersed phase in PP-2/PA-1 blends containing 5% ionomer are shown in Fig. 2b, as a function of polyamide concentration. Larger particle sizes are also observed at higher concentrations of the dispersed phase. In addition, the compatibilizer has resulted in particle dimensions which are considerably smaller than those observed for the un-

compatibilized PP-2/PA-1 blends, over the entire composition range. Photomicrographs of microtomed surfaces illustrating this effect are shown in Fig. 1. The values of the polydispersity given in Table II are also smaller than those found for the uncompatibilized PP-2/PA-1 blends, particularly at small dispersed phase concentrations.

As shown in Fig. 3, similar trends were found for the PE-1/PA-1 blends, containing 0% and 5% ionomer. However, at high minor phase concentrations, the particle dimensions are smaller than those observed for the PP-2/PA-1 blends. This is particularly true for the volume average diameter. As shown in Table II, the uncompatibilized PE-1/PA-1 blends are less polydispersed than the uncompatibilized PE-2/PA-1 blends. However, once the interface is modified, differences in the polydispersities of the two blends are minor until the region of dual phase continuity is approached. It is interesting to note that if the particle size is lower at low composition, the entire curve is shifted. This result was reported previously for polypropylene/polycarbonate systems [25] and has been discussed in detail in a previous paper [39].

By comparing the particle size of the uncompatibilized blends with that measured for the blends containing 5% ionomer, it is possible to observe the extent of particle size reduction. This is illustrated in Fig. 4. Overall, the particle size reduction is quite similar for the two blend systems, where  $d_v(0\%)/d_v(5\%)$  is 3.6 for

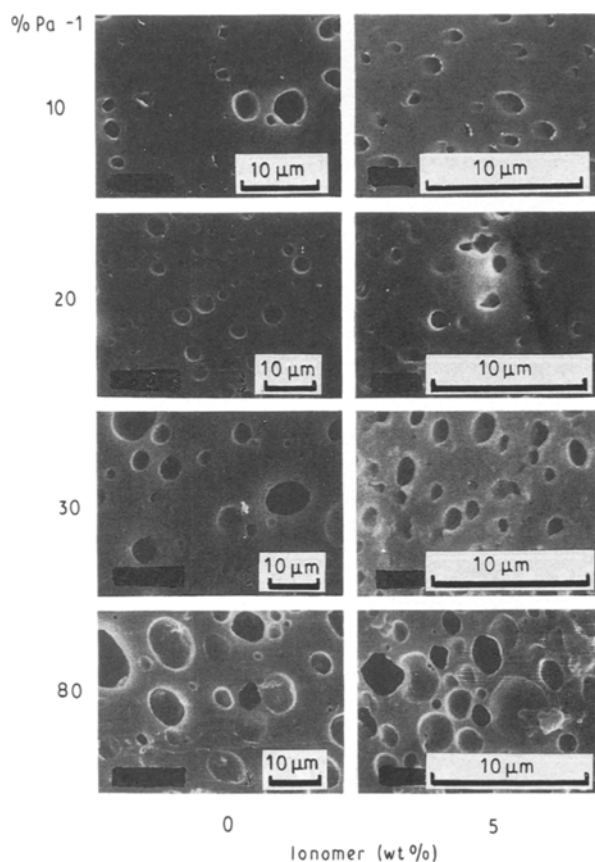


Figure 1 SEM photomicrographs of the microtomed/etched surfaces of PP-2/PA-1 blends containing 0% and 5% ionomer by weight on the minor phase.

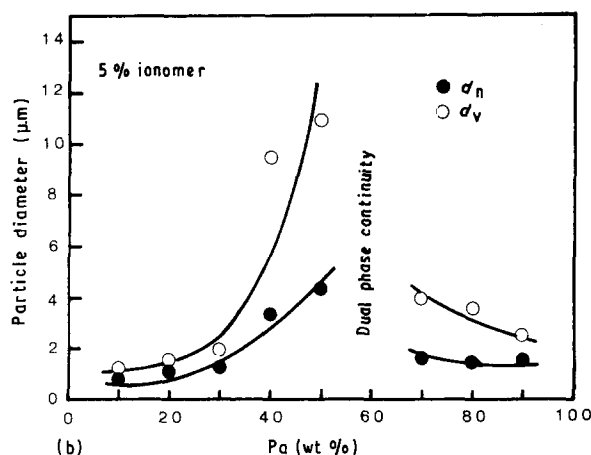
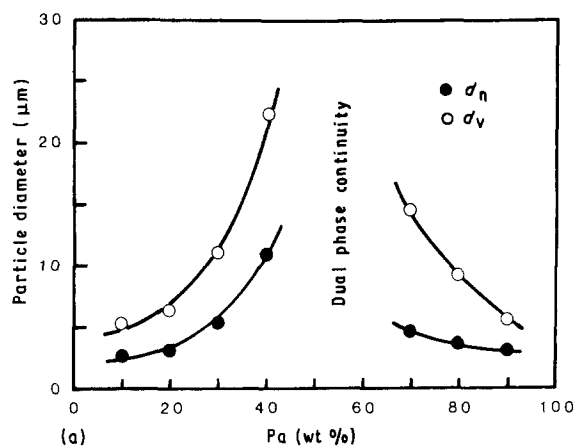


Figure 2 Composition dependence of the size of the dispersed phase in PP-2/PA-1 blends containing (a) 0% ionomer and (b) 5% ionomer, based on the weight of the minor phase.

TABLE II The polydispersity of particle sizes ( $d_w/d_n$ ) as a function of blend composition, for the uncompatibilized and compatibilized PP-2/PA-1 and PE-1/PA-1 blends

Weight %PA	PP-2/PA-1		PE-1/PA-1	
	0% ionomer	5% ionomer	0% ionomer	5% ionomer
10	2.0	1.6	1.5	1.5
20	2.1	1.4	1.8	1.5
30	2.1	1.6	1.8	1.7
40	2.0	2.8	1.5	1.8
70	3.2	2.5	1.6	1.6
80	2.5	2.3	1.5	1.6
90	1.8	1.6	1.7	2.1

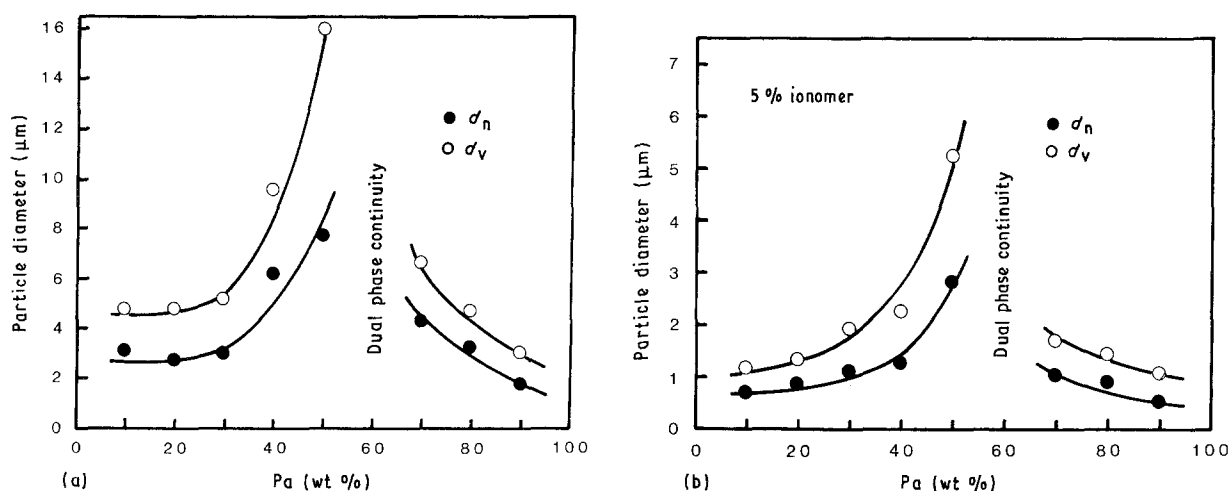


Figure 3 Composition dependence of the size of the dispersed phase in PE-1/PA-1 blends containing (a) 0% ionomer and (b) 5% ionomer, based on the weight of the minor phase.

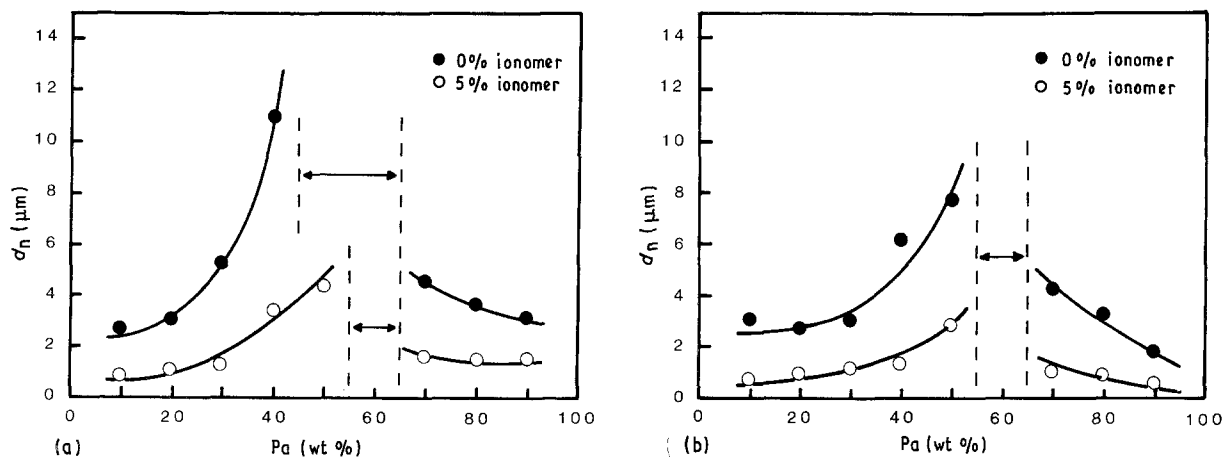


Figure 4 Comparison between the particle size of the uncompatibilized blend and that of the blend containing 5% ionomer, as a function of polyamide content for (a) PP-2/PA-1 and (b) PE-1/PA-1. The arrows designate the regions of dual phase continuity.

PP/PA and 3.5 for PE/PA. However, the ionomer causes a greater reduction in the size of dispersed polyamide (4.4) than dispersed polyolefin (3.1). This effect has previously been interpreted as the result of the greater affinity which occurs between the ionomer and the polyamide than between the ionomer and the polyolefins [28, 29]. Fourier transform infrared spectroscopic studies have shown that amidation occurs between the NH groups of the polyamide and the CO functionalities of the ionomer [29]. It is evident that the presence of the ionomer in the polyolefin/polyam-

ide blends improved the adhesion between the dispersed phase and the matrix as a result of interactions occurring across the interface. This effect can more readily be observed visually in Fig. 5 for the 80% PE-1/20% PA-1/5% ionomer blend, where the matrix is strongly adhering to the dispersed phase.

During the mixing process, the dispersed phase experiences a combination of both particle breakup and coalescence. According to Taylor [40, 41], a droplet of a Newtonian dispersed phase in a Newtonian matrix will undergo deformation and breakup as

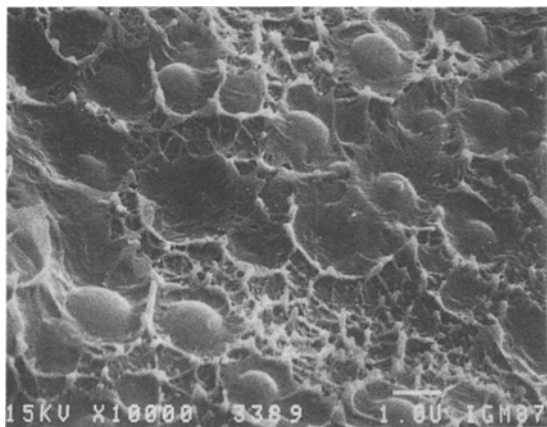


Figure 5 SEM photomicrograph of the fracture surface of the 80% PE-1/20%PA-1/5% ionomer blend.

long as the total force acting on the particle is greater than the surface tension. Taylor defined a dimensionless variable,  $W_e$ , such that

$$W_e = \eta_m r \dot{\gamma} / \gamma_{12} \quad (1)$$

where  $r$  is the particle radius,  $\eta_m$  is the viscosity of the matrix,  $\dot{\gamma}$  is the shear rate and  $\gamma_{12}$  is the interfacial tension. From Equation 1, it is evident that there is a critical value of  $W_e$  below which particle deformation will no longer occur, which in turn coincides with a critical value of the particle size. Taylor's criterion [40, 41] for the smallest particle size which can result during particle breakup corresponds to  $W_e = 0.5$ , or  $r_c = \gamma_{12} / 2 \eta_m \dot{\gamma}$ . For the 90%PP/10%PA blend, the value of the system parameter,  $\eta_m \dot{\gamma} / \gamma_{12}$ , was determined as  $2.34 \mu\text{m}^{-1}$ , using a value of  $100 \text{ s}^{-1}$  as the shear rate and  $1.35 \times 10^{-2} \text{ Nm}^{-1}$  as the interfacial tension [42]. The critical value of the radius is thus  $0.21 \mu\text{m}$ . This is much smaller than the average radius ( $1/2 d_n$ ) measured for this blend,  $1.34 \mu\text{m}$ .

Tokita [43] developed a relationship for the equilibrium particle size,  $r^*$ , which results when the particle deformation and coalescence phenomena are balanced:

$$r^* = \frac{\gamma_{12}}{\eta_m \dot{\gamma}} \frac{12 P \phi_d + 48 P^2 \phi_d^2 E_{dk}}{\pi^2 \eta_m \dot{\gamma}} \quad (2)$$

where  $\phi_d$  is the volume fraction of the dispersed phase,  $P$  is the probability that two particles that have collided will result in coalescence, and  $E_{dk}$  is the macroscopic bulk breaking energy. In order for particle breakup to occur,  $\eta_m \dot{\gamma}$  must exceed  $E_{dk}$ . This equation is very similar to Taylor's, Equation 1, since it predicts an inverse relationship between the droplet radius and the system parameter,  $\eta_m \dot{\gamma} / \gamma_{12}$ . Moreover, this equation takes into account the effect of composition on the dispersed phase size.

The applicability of Tokita's theory is limited because the probability of particle-particle collision resulting in coalescence is unknown. It is also difficult to estimate the value of the bulk breaking energy. Recently, Elmendorp and Vander Vegt [35] have shown that interparticle collisions have a greater probability of resulting in coalescence if the dispersed phase is small and if the interface is highly mobile.

Thus coalescence probability decreases rapidly with increasing  $W_e$  and is zero when  $W_e > 3.5$ .

The similarities between interfacially modified polymer blends and stabilized oil/water or oil/oil emulsions have previously been addressed by Willis and Favis [28] as well as by Fayt *et al.* [44, 45] and Periard and Reiss [46]. In both cases, the size of the dispersed phase decreases as the concentration of emulsifier [47] or compatibilization agent [28, 45, 46] increases until the interface between the two phases is saturated. At this point an equilibrium particle size is observed. The localization of surfactant at the interface reduces the mobility or the tangential motion of the interface due to the formation of interfacial tension gradients [48]. In oil/water emulsions, the size of the dispersed phase increases only slightly with dispersed phase volume fraction, particularly if the surfactant concentration remaining in the continuous phase after emulsification is constant [48]. Thus, in such systems where the phase size does not change significantly with composition, it is the interfacial area that determines the emulsion properties. Near the phase inversion region, whether it arises from changes in temperature or composition, emulsions become unstable. As a result, an increase in coalescence [49] and a decrease in viscosity [50] can occur. In this respect, the dependence of phase size on the composition of compatibilized polyolefin/polyamide blends resembles the behaviour of stabilized emulsions. As shown in Fig. 4, there is but a slight increase in the phase size with composition up to 30–40% by weight of dispersed phase. As the phase inversion region is approached, the particle size increases more rapidly due to an increase in coalescence. In the compatibilized blend, decreased mobility at the interface results in fewer particle-particle contacts, and hence less coalescence is observed with increasing composition. Coalescence for an immobilized blend only becomes significant when the composition of the minor phase is so high that physical impingement occurs. At this point, near the region of dual phase continuity, the dependence of phase size on composition is very high. In summary, the interfacial modification of polyolefin/polyamide blends significantly diminishes the influence of composition on phase size as compared to the uncompatibilized case. It is only near the region of dual phase continuity that compatibilized blends show a much more pronounced dependence on phase size.

### 3.2. Phase inversion

In Fig. 4, it is possible to see that the region of dual phase continuity occurs at approximately 60% polyamide by weight for each blend. For the PP-2/PA-1 blends, the presence of the ionomer has reduced the width of the region of dual phase continuity. The same effect was not observed for the PE-1/PA-1 blend, but may in fact be occurring within the 10% concentration unit interval used in this composition study. The transition from a polyamide dispersed phase to a polyamide matrix can be observed in Figs. 6 and 7 from the SEM photomicrographs of cryogenically fractured surfaces of PP-2/PA-1 and PE-1/PA-1

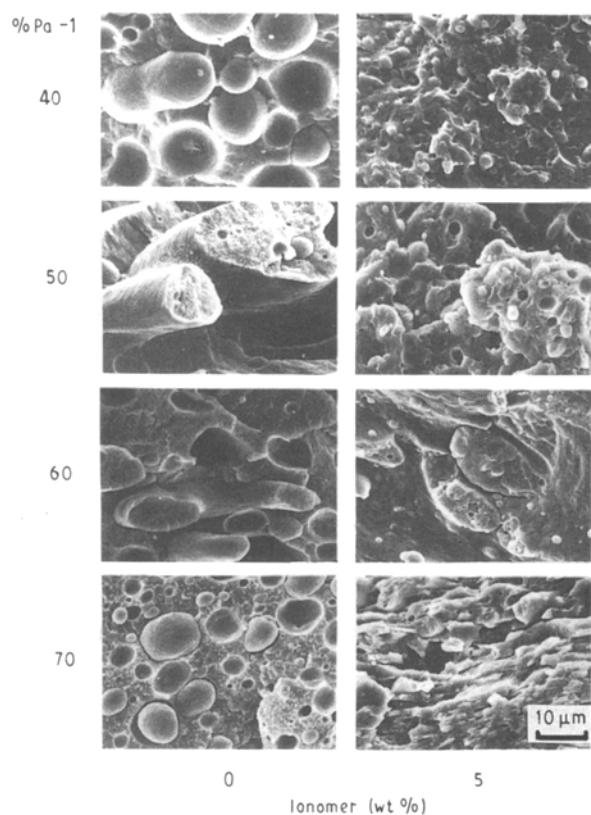


Figure 6 SEM photomicrographs of the fracture surfaces of the PP-2/PA-1 blends containing a 0% and 5% ionomer by weight on the minor phase.

blends, containing 0% and 5% ionomer by weight. A narrowing of the region of dual phase continuity for the compatibilized blend is also consistent with an explanation based on reduced interfacial mobility. In such a system, as explained above, coalescence effects would be suppressed up to the region of phase inversion where physical encroachment occurs.

According to Jordhamo *et al.* [51], the point of phase inversion can be predicted from,

$$\frac{\eta_d \phi_m}{\eta_m \phi_d} = 1 \quad (3)$$

where  $\eta_d$  and  $\eta_m$  represent the viscosities of the dispersed phase and the matrix, respectively, and  $\phi_d$ ,  $\phi_m$ , the corresponding volume fractions for phase inversion. By substituting torque ratios for viscosity ratios, the predicted values of the polyamide volume fraction at phase inversion were calculated as 0.50 and 0.59 for the PP-2/PA-1 and PE-1/PA-1 blends, respectively. These values correspond to 56% and 65% polyamide by weight, respectively. From Fig. 4, it can be seen that the predicted regions of dual phase continuity are encompassed by the observed regions. It should be noted that this relationship does not always hold. In polypropylene/polycarbonate blends, where the phase size/composition relationship was studied for two systems of widely different viscosity ratio, significant deviation was found between the predictions made using Equation 3 and experimental observations [25].

The torques measured for the PP-2/PA-1 and PE-1/PA-1 blends during melt mixing in the Brabender

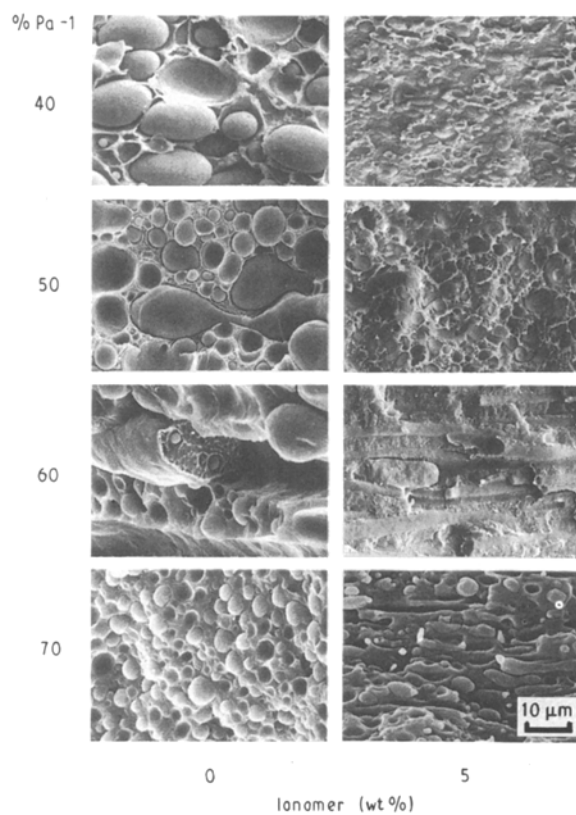


Figure 7 SEM photomicrographs of the fracture surfaces of the PE-1/PA-1 blends containing a 0% and 5% ionomer by weight on the minor phase.

mixing chamber are shown in Fig. 8, as a function of polyamide concentration. For both uncompatibilized blend systems, negative deviations occur between the measured values of the torque and the tie-line joining the torques of the pure components. This type of torque/composition curve is characteristic of an incompatible blend [52]. The absence of interfacial interactions between the components of such a blend generally results in interlayer slip during the blending process [53].

When the ionomer compatibilizer is added to these blends, an increase in the measured torques is observed over the entire composition range. It has previously been shown that the ionomer improves interfacial interactions in polyolefin/polyamide blends [28, 29]. Thus, these results indicate that the localization of the ionomer at the interface has decreased the interfacial mobility at all dispersed-phase contents.

For both uncompatibilized and compatibilized blends, the minimum torque values appear at approximately 60% polyamide. This composition corresponds to the region where dual phase continuity was observed. At this point, the interfacial area is at a maximum and as a result, the blend experiences the most interlayer slip. For the case of polycarbonate/polypropylene blends [25], the region of phase inversion was also found to correspond to the point where the torque measured for the blend displayed a maximum deviation from the additivity line.

The observations made for the compatibilized polyolefin/polyamide blends, in terms of (a) the diminished influence of blend composition on dispersed phase

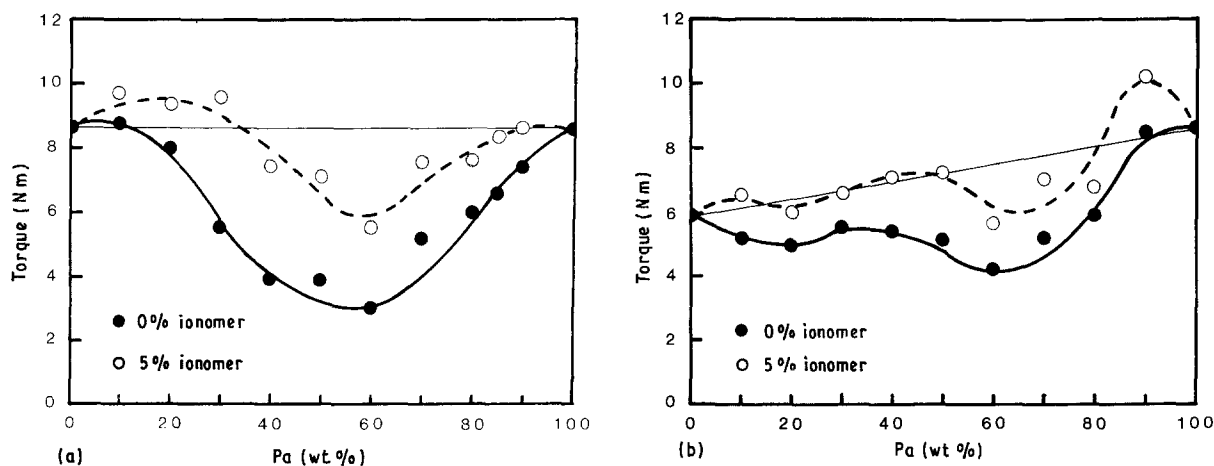


Figure 8 Composition dependence of the torque measured for (a) PP-2/PA-1 and (b) PE-1/PA-1 blends containing 0% and 5% ionomer by weight on the minor phase.

size, (b) the more rapid rise in phase size with composition near the region of dual phase continuity, and (c) the narrowing of the region of dual phase continuity, are consistent with predictions made for an interface characterized by a lower mobility. The increase in the measured torque due to compatibilization, as shown in Fig. 8, demonstrates the reduction in interfacial mobility. As a result, these observations correlate quite well with classical emulsion studies.

### 3.3. Influence of interfacial modification on the role of the viscosity ratio

Several PP/PA and PE/PA blends having a 10% dispersed phase concentration were prepared over a ten-fold range of torque ratios (0.32 to 3.16). It may be mentioned that the value of the shear stress ( $\eta_m \dot{\gamma}$ ) was not constant over the range of torque ratios studied. However, Favis and Chalifoux [26] have demonstrated the influence of shear stress on phase size in non-compatibilized blends to be small. For each blend, the addition of ionomer resulted in an average 13% increase in the torque measured during melt blending. More importantly, the average increase in the torque was greater for dispersed polyolefins (15%) in comparison to dispersed polyamide (9%). This is expected because of the strong affinity which the ionomer has for the polyamide, as discussed elsewhere [28, 29]. In addition, it may be noted that the small quantity of ionomer present in these blends (0.5% by weight of blend) has a negligible effect on the value of the torque ratio of the blend.

The number average diameters determined from the microtomed/etched surfaces of blends containing dispersed polyamide and dispersed polyolefins, are shown as a function of torque ratio in Figs. 9 and 10, respectively. It is evident that there is an increase in the particle size as the viscosity of the dispersed phase increases with respect to the viscosity of the matrix. This is in accordance with the theory developed by Taylor for Newtonian systems [40, 41], as well as other studies of the dependence of polymer blend morphology on torque or viscosity ratio [18, 26, 38, 54].

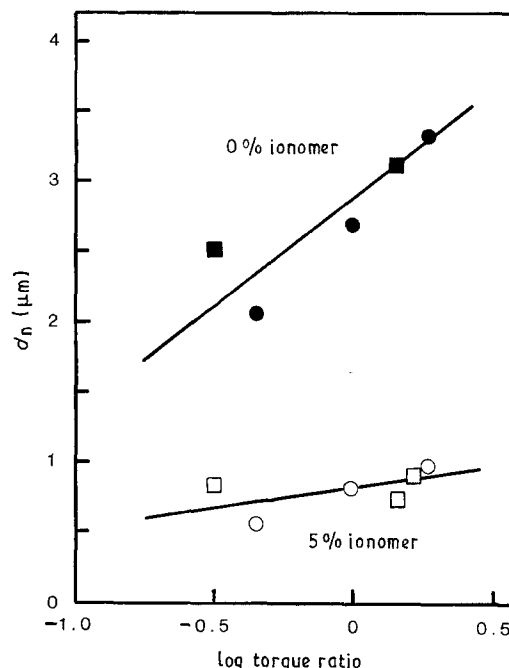


Figure 9 Dependence of the number average diameter on the torque ratio of the blends containing 10% polyamide dispersed in a polypropylene (●○) or polyethylene (■□) matrix, with 0% and 5% ionomer by weight.

The addition of ionomer to the PP/PA and PE/PA blends resulted in smaller dispersed phase sizes in comparison to the uncompatibilized blends, over the entire range of torque ratios studied. It is interesting to note that a more extensive particle size reduction occurs for the blends that have larger torque ratios. This is particularly true for the blends containing a dispersed polyethylene phase, where  $d_n(0\%)/d_n(5\%)$  is 3.1 at  $\log(\text{torque ratio})$  of 0.5, while a value of 1.3 was found at  $-0.5$ . It is also evident that the compatibilization has significantly reduced the dependence of the phase size on the torque ratio of the blend. The same trend was observed by Wu [55] for a compatibilized polyamide/elastomer blend in comparison to the uncompatibilized blend. The shift observed for the dispersed PP data in Fig. 10 is consistent with the reduction in the interfacial tension of

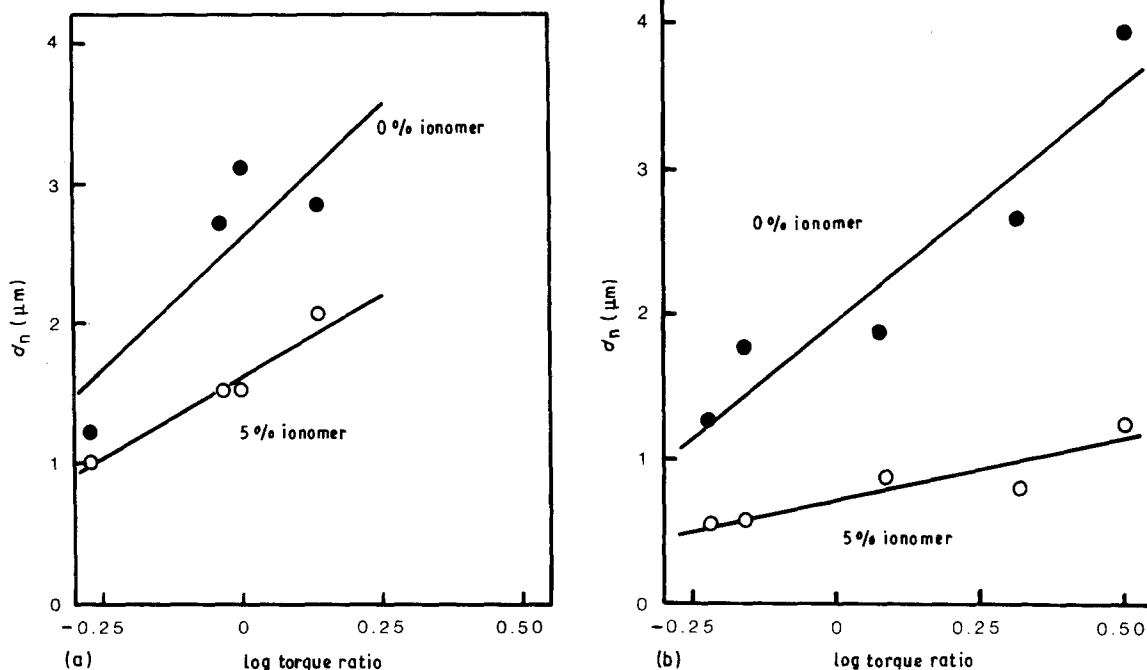


Figure 10 Dependence of the number average diameter on the torque ratio of the blends containing (a) 10% dispersed polypropylene and (b) 10% dispersed polyethylene, with 0% and 5% ionomer by weight.

the blend due to the presence of the ionomer. However, the diminished dependence of the phase size on the viscosity ratio observed for the dispersed PA and dispersed PE shown in Figs. 9 and 10 is more difficult to explain. It is possible that as the particle size is reduced to such an extent that it approaches the critical value predicted by Taylor's theory [40, 41] (calculated as  $0.21 \mu\text{m}$  for the PP-2/PA-1 blend), the deformation and breakup of the dispersed phase becomes increasingly difficult. Under these conditions, the influence of the torque ratio of the blend on phase size becomes less important. The influence of interfacial modification has therefore diminished the dependence of phase size on the viscosity ratio of the blend.

#### 4. Concluding remarks

From the results presented, it is evident that the ionomer has a moderating effect on the morphology of the blends. The size of the dispersed phase in compatibilized blends is only slightly dependent on the blend composition (below 30–40% dispersed phase content). Near the region of dual phase continuity, the dependence becomes very pronounced. In fact, for the PP/PA blend, the region of dual phase continuity became narrower when ionomer was added. These observations concur with classical emulsion studies and are consistent with an explanation based on reduced interfacial mobility. There is also a less dramatic dependence of phase size on the torque ratio (viscosity ratio) of the blend, in comparison with that observed for uncompatibilized blends. It is suggested that this observation may be explained from Taylor's theory [40, 41] which states that it is more difficult to break up a smaller particle than a larger one.

#### Acknowledgements

We sincerely appreciate the assistance of F. Hamel with the blend preparations, and D. Simard and M. Thibodeau with the scanning electron microscopy.

#### References

1. R. J. M. BORGGREVE, R. J. GAYMANS, J. SCHUIJER and J. F. INGEN HOUZ, *Polymer* **28** (1987) 1489.
2. S. Y. HOBBS, R. C. BOPP and V. H. WATKINS, *Polym. Engng. Sci.* **23**(7) (1983) 380.
3. S. CIMMINO, F. COPPOLA, L. D'ORAZIO, R. GRECO, G. MAGLIO, M. MALINCONICO, C. MANCARELLA, E. MARTUSCELLI and G. RAGOSTA, *Polymer* **27** (1986) 1874.
4. B. Z. JANG, D. R. UHLMANN and J. B. VANDER SANDE, *J. Appl. Polym. Sci.* **30** (1985) 2485.
5. S. WU, *Polymer* **26** (1985) 1855.
6. J. SILBERBERG and C. D. HAN, *J. Appl. Polym. Sci.* **22** (1978) 599.
7. A. M. DONALD and E. J. KRAMER, *J. Mater. Sci.* **17** (1982) 1765.
8. S. Y. HOBBS, *Polym. Engng. Sci.* **26**(1) (1986) 74.
9. B. Z. JANG, D. R. UHLMANN and J. B. VANDER SANDE, *Polym. Engng. Sci.* **5**(10) (1985) 643.
10. C. B. BUCKNALL, F. F. P. COTE and I. K. PARTRIDGE, *J. Mater. Sci.* **21** (1986) 301.
11. C. B. BUCKNALL in "Polymer blends", Vol. 2, edited by D. R. Paul and S. Newman, (Academic Press, New York, 1978).
12. S. NEWMAN *ibid.*
13. R. P. KAMBOUR, *J. Polym. Sci., Macromol. Rev.* **7** (1973) 154.
14. H. KESKKULA in "Polymer compatibility and incompatibility: principles and practice", Vol. 2, MMI Symposium, edited by K. Sole (Harwood, New York, 1982).
15. D. YANG, B. ZHANG, Y. YANG, Z. FANG, G. SUN and Z. FENG, *Polym. Engng. Sci.* **24**(8) (1984) 612.
16. R. GRECO, M. MALINCONICO, E. MARTUSCELLI, G. RAGOSTA and G. SCARINZI, *Polymer* **28** (1987) 1185.
17. P. GALLI, S. DANESI and T. SIMONAZZI, *Polym. Engng. Sci.* **24**(8) (1984) 544.
18. J. KARGER-KOCSIS, A. KALLO and V. N. KULEZNEV, *Polymer* **25** (1984) 279.
19. P. M. SUBRAMANIAN, *Polym. Engng. Sci.* **25**(8) (1985) 483.



20. P. VAN GHELUWE, B. D. FAVIS and J. P. CHALIFOUX, *J. Mater. Sci.* **23** (1988) 3910.
21. P. M. SUBRAMANIAN, *Polym. Engng. Sci.* **27(20)** (1987) 1574.
22. P. M. SUBRAMANIAN and V. MEHRA, *Polym. Engng. Sci.* **27(9)** (1987) 663.
23. P. M. SUBRAMANIAN, *Int. Polym. Process.* **3(1)** (1988) 33.
24. M. R. KAMAL, I. A. JINNAH and L. A. UTRACKI, *Polym. Engng. Sci.* **24(17)** (1984) 1337.
25. B. D. FAVIS and J. P. CHALIFOUX, *Polymer* **29(1988)** 1761.
26. B. D. FAVIS and J. P. CHALIFOUX, *Polym. Engng. Sci.* **27(20)** (1987) 1591.
27. B. D. FAVIS, *J. Appl. Polym. Sci.*, **39** (1990) 285.
28. J. M. WILLIS and B. D. FAVIS, *Polym. Engng. Sci.* **28(21)** (1988) 1416.
29. J. M. WILLIS, C. LAVALLÉE and B. D. FAVIS, submitted to *J. Mater. Sci.*
30. D. BRAUN and U. EISENLOHR, *Kunststoffe* **65** (1975) 139.
31. L. A. UTRACKI, M. M. DUMOULIN and P. TOMA, *Polym. Engng. Sci.* **26(1)** (1986) 34.
32. P. M. SUBRAMANIAN, U.S. Patent 4444817 (1984).
33. P. M. SUBRAMANIAN, U.S. Patent 4410482 (1983).
34. C. C. CHEN, E. FONTAN, K. MIN and J. L. WHITE, *Polym. Engng. Sci.* **28(2)** (1988) 69.
35. J. J. ELMENDORP and A. K. VANDER VEGT, *ibid.* **26(19)** (1986) 1332.
36. D. HEIKENS and W. BARENTSEN, *Polymer* **18** (1977) 69.
37. D. HEIKENS, N. HOEN, W. BARENTSEN, P. PIET and H. LADAN, *J. Polym. Sci., Polym. Symp.* **62** (1978) 309.
38. K. MIN, J. L. WHITE and J. F. FELLERS, *Polym. Engng. Sci.* **24(17)** (1984) 1327.
39. B. D. FAVIS and J. M. WILLIS, *J. Polym. Sci., Polym. Physics*, **28** (1990) 2259.
40. G. I. TAYLOR, *Proc. R. Soc.* **A146** (1934) 501.
41. G. I. TAYLOR, *Proc. R. Soc.* **A138** (1934) 41.
42. S. WU, in "Polymer interface and adhesion" (Marcel Dekker, New York, 1982).
43. N. TOKITA, *Rubber Chem. Technol.* **50** (1977) 292.
44. R. FAYT, R. JEROME and Ph. TEYSSIE, *J. Polym. Sci., Polym. Lett.* **24** (1986) 25.
45. R. FAYT, R. JEROME and Ph. TEYSSIE, *Makromol. Chem.* **187** (1986) 837.
46. J. PERIARD and G. RIESS, *Colloid Polym. Sci.* **253** (1975) 362.
47. L. DJAKOVIC, P. DOKIC, P. RADIVOJEVIC, I. SEFER and V. SOVILIJ, *Colloid Polym. Sci.* **265** (1987) 993.
48. P. WALSTRA in "Encyclopaedia of emulsion technology", Vol. 1, edited by P. Becher (Marcel Dekker, New York, 1983) Ch. 2.
49. K. SHINODA and H. SAITO, *J. Colloid Interf. Sci.* **30(2)** (1969) 258.
50. P. SHERMAN, *J. Soc. Chem. Ind.* **69(2)** (1950) S70.
51. G. M. JORDHAMO, J. A. MANSON and L. H. SPERLING, *Polym. Engng. Sci.* **26(8)** (1986) 517.
52. C. D. HAN, in "Multiphase flow in polymer processing" (Academic Press, New York, 1981).
53. L. A. UTRACKI, *Polym. Engng. Sci.* **23(11)** (1983) 602.
54. W. BERGER, H. W. KAMMER and C. KUMMERLOWE, *Makromol. Chem., Suppl.* **8** (1984) 101.
55. S. WU, *Polym. Engng. Sci.* **27(5)** (1987) 335.

*Received 6 March  
and accepted 6 July 1990*